Environmental Science Processes & Impacts

ROYAL SOCIETY OF CHEMISTRY

PAPER

View Article Online
View Journal | View Issue

Cite this: *Environ. Sci.: Processes Impacts*, 2025, **27**, 1629

Longevity of size-dependent particle removal performance of do-it-yourself box fan air filters†

Theresa Pistochini, [ab] Graham Jaeger,[bc] Christopher D. Cappa [a] and Richard L. Corsi*[a]

Filtration performance of do-it-yourself (DIY) box fan filters deployed across a university campus was assessed over an academic year. Four DIY air filters were constructed from box fans and air filters with a minimum efficiency reporting value (MERV) of 13 and deployed in four spaces (two laboratories that include sources of particles and two offices). They were operated 9 hours daily with a programmable timer and were continuously monitored with power meters. Particle concentrations in the spaces were continuously monitored with low-cost nephelometers. The particle size dependent clean air delivery rate (CADR) and single pass filtration efficiency for each box was measured in a laboratory before deployment and every 10 weeks, for a total of five measurements over 40 weeks. We find that these DIY box fan filters maintain robust performance over time, with each air filter maintaining at least 60% of its initial CADR at the end of the 40 week study even with daily operation in environments with modest particle concentrations. CADR values for particles of 1.0–3.0 μm optical diameter averaged 34% higher than CADR values for 0.35–1.0 μm particles, aligning with MERV 13 filter size-dependent filtration expectations. Reductions in CADR over time were attributed to a reduction in filtration efficiency, likely due to a loss of filter electrostatic charge over time. There was no strong indication that increased resistance due to particle accumulation on filters appreciably decreased flow rates over time for any of the fans. The long-term robustness of DIY box fan air filters demonstrates their validity as a cost-effective, high performance, alternative to portable high efficiency particulate air (HEPA) filters.

Received 6th July 2024
Accepted 21st October 2024

DOI: 10.1039/d4em00406j

rsc.li/espi

Environmental significance

The work provides insight into the ability of low-cost do-it-yourself (DIY) air filters to improve the indoor environment by reducing particle concentrations and related human exposure. The longterm and size-dependent performance is studied to enable analysis of how DIY air filters will perform with regards to particles generated by different sources (e.g. wildfire smoke *vs.* respiratory aerosols)

Introduction

Filtration of indoor air with portable air filters reduces particle concentrations indoors, which is expected to have health benefits for building occupants.[1] Most portable air cleaners that are applied in intervention studies use high efficiency particulate air (HEPA) filters that remove 99.97% of the most penetrating particles from the airstream.[2] Low-cost do-it-yourself portable air cleaners can be built from a box fan and standard filters used in heating, ventilation, and air conditioning (HVAC) systems, which are rated based on their minimum efficiency reporting value (MERV). When MERV-rated filters are arranged in a box configuration, termed a Corsi–Rosenthal box (CR box), the airflow resistance is low, the airflow rates are high, and the particle removal rates exceed most commercially available portable HEPA filters.[3] While the fraction of particles removed on a single-pass through a MERV-rated filter is lower than a HEPA filter, the overall filtration performance can be compared through a clean air delivery rate (CADR) metric, which is a measure of the volumetric rate of particle-free air delivered by the air cleaner.[4]

Portable filtration has been observed to reduce the concentration of respiratory aerosols and the risk of respiratory infection transmission between occupants in a variety of building types. In a field study in 16 homes with an individual positive for COVID-19, Myers *et al.* observed a reduction in SARS-CoV-2 RNA positive air samples in the room most often occupied by the infected individual when a portable HEPA filter was

[a]*Department of Civil and Environmental Engineering, University of California Davis, 1 Shields Avenue, Davis, CA, USA. E-mail: rlcorsi@ucdavis.edu*

[b]*Western Cooling Efficiency Center, University of California Davis, 215 Sage Street, Suite 100, Davis, CA, USA*

[c]*Department of Mechanical and Aeronautical Engineering, University of California Davis, 1 Shields Avenue, Davis, CA, USA*

† Electronic supplementary information (ESI) available. See DOI: https://doi.org/10.1039/d4em00406j

operated.[5] In a field study of a hospital patient room and adjacent corridor and nurses' station, Buising *et al.* demonstrated that a surrogate for respiratory aerosol rapidly travelled from the patient room to adjacent spaces and that portable HEPA filters increased aerosol removal rates and decreased spread outside the patient room.[6] In a field study in a secondary school with 90 students, Banholzer *et al.* found that air samples positive for SARS-CoV-2 were reduced from 8% to 5% when a portable HEPA filter was operated in classrooms.[7] Additionally, average viral concentrations of positive air samples were substantially reduced by operation of the HEPA filter. Although the infection transmission risk odds ratio for SARS-CoV-2 was calculated to be comparable for the periods with and without portable air filters, the short two-week intervention and low number of infections resulted in high uncertainty in this conclusion. In a six-month study comparing two daycare centres with a portable HEPA filter intervention to a large reference population, Vartiainen *et al.* demonstrated that absenteeism due to child illness was reduced by 32% in the daycare centres with HEPA filters.[8] These field results are consistent with infection transmission risk modelling that predicts a reduced number of infections when using air filters that remove respiratory aerosols from the indoor air.[8,9]

Filtration has additional health benefits in reducing occupant exposure to particles including pollen, pet dander, indoor cooking generated particle pollution, and outdoor-source particle pollution (*e.g.* vehicle exhaust, forest fire and residential wood smoke). A general review of the health benefits of particle filtration by Fisk in 2013 concluded that the majority of well-designed intervention studies employing particle filtration report modest statistically significant improvements in health, particularly for people with allergies or asthma. Notably, two of the studies reviewed demonstrated portable HEPA filtration used in homes reduced both particulate matter exposure and health markers (vascular and endothelial function) that are predictors of future coronary events.[10,11] A 2021 review of 21 papers related to portable air cleaners and published between 2005 and 2020 by Cheek *et al.* showed substantial reductions (22 to 90%) of indoor particulate matter less than 2.5 microns (PM2.5) when portable air filters were in use.[1] Health benefits of reduced particulate matter exposure assessed by these studies were also summarized, but evidence of benefits was limited and inconsistent. However, the authors note that the cumulative body of scientific evidence supports that there are positive health benefits associated with reduced PM2.5 exposure.

A limitation of the widespread deployment of portable HEPA filters is cost. In a cost-benefit analysis of HEPA filtration in 2017, Fisk and Chan estimated the cost of procuring HEPA filtration for a home at \$0.55 to \$1.40 per m^3 h^{-1} of clean air delivered (CADR) and determined that the mortality-related economic benefits exceed the cost of purchasing and operating air cleaners when used over their multi-year life.[12] In 2022, Dal Porto *et al.* estimated the cost of HEPA filtration at \$0.44 to \$0.51 per m^3 h^{-1} of CADR.[3] The American Home Appliance Manufacturers (AHAM) recommend a CADR target of 12 m^3 h^{-1} per m^2 of floor area, which equates to \$5.39 to \$6.25 per m^2 of floor area when applying costs from Dal Porto *et al.*[13] Therefore, HEPA filtration may not be a priority or may be too costly for some residents and operators of commercial buildings (*e.g.* schools, daycares, offices). The CR box offers a first-cost that is an order of magnitude below HEPA at \$0.05 to \$0.07 per m^3 h^{-1} of CADR.[3] While multiple papers have been published documenting the filtration performance of new CR boxes,[3,14–18] there is no published data on the longevity of the devices and their long-term performance. The purpose of this research was to assess the filtration performance of CR boxes operated daily over a 9 month academic year to determine how well these low-cost do-it-yourself filters perform over time.

Experimental

Four CR boxes were constructed, tested in new condition, and deployed across the UC Davis campus where their use was continuously monitored *via* power measurement. The CR boxes were collected every 10 weeks, retested, and redeployed for a total of 40 weeks of operation and five performance measurements. Each round of testing included measurement of the particle-size dependent CADR and single pass filtration efficiency (SPFE).

Construction

Four CR boxes were constructed with the following materials each: three-speed box fan (Lasko model 3129342), 5 cm deep MERV 13 filters (two 50 × 50 cm and two 40 × 50 cm), cardboard shroud with opening of diameter 42 cm to reduce backflow through the corners of the fan, cardboard base, and duct tape. Filters for box 1 were from Air Handler (AH) and filters for boxes 2–4 were from Tex-Air (TA). Although both brands of filters had the same MERV 13 filtration efficiency rating, the filters looked visibly different, with the AH filters having a fuzzier appearance. The cost of each CR box was approximately \$70 (\$24 fan, \$11 × 4 filters, \$2 duct tape), consistent with the cost reported by Dal Porto *et al.*[3]

Deployment and long-term monitoring

The CR boxes were deployed in four locations across the UC Davis campus, two lab environments and two office spaces (Table 1). Ventilation with 100% outside air (OA) and activities occurring in the selected labs were expected to be large sources of particles to load the CR boxes. The Bainer laboratory is used primarily as a teaching laboratory for several undergraduate civil and environmental engineering courses and also as a general workshop space with a variety of sporadic activities (cutting, drilling, hand tools) that may generate particles. Within the Western Cooling Efficiency Center (WCEC) research laboratory particles were periodically generated from typical shop activities (cutting and drilling wood and metal).

Power

Power draw of each CR box was continuously measured and logged every 5 minutes by an Onset HOBO Plug Load Data Logger (UX120-018). Power data was used to determine run time at each fan speed and assess changes in the power draw for

Table 1 Deployment locations for four CR boxes on the UC Davis campus

CR box	Space	Building ventilation type	Ventilation schedule
1	Bainer – lab	100% OA	All hours
2	WCEC – lab	Local exhaust	Varies (manual)
3	Kemper – office	100% OA	All hours
4	Ghausi – office	Recirculated	M–F 6:00–18:00

a particular speed over time. A digital programmable timer turned on the fan daily at 8:00 and off at 17:00. The users could change the fan speed (low, medium, high) to suit their preference but were asked to leave the fan turned on (so that the on–off status would be controlled by the timer). The power used by the timer (about 1 W) was included in the power measurements. The change in power over time was assessed with a linear fit of the power data when the fan was running.

Clean air delivery rate (CADR)

The CADR was calculated from the measured decay of salt particles in a room with and without the CR box operating. The methods generally followed Dal Porto *et al.*[3] The salt particles were generated using a portable mesh nebulizer (Wellue or equivalent) using an aqueous table salt solution (50 g L^{-1}).

Measurements were conducted in a conference room at WCEC with measured volume of 120 m^3 (Fig. 1). The mechanical heating, cooling, ventilation and filtration system for the conference room was shut off so that the only particle loss mechanisms in the room were deposition, air exchange through infiltration, and removal by the CR box. The total particle loss rate for combined deposition and infiltration was measured without the CR box operating. This loss rate was subtracted from the particle loss rate calculated with the CR box operating to obtain the particle loss rate attributable to the CR box.

The following procedure was used to collect the data required to calculate the CADR:

Fig. 1 CR box experimental test setup in a conference room.

1. Salt particles were generated for 10 minutes while the CR box was off. Two fans placed on the table mixed the room air at low speed during this period.

2. The mixing fans were turned off. The room was left undisturbed for 10 minutes.

3. The CR box was turned on for 30 minutes to measure the exponential decay of the particles.

In the first round of testing, particle concentrations by size bin were measured every 5 seconds with two types of instruments, a laboratory-grade aerodynamic particle sizer (APS; TSI model 3321) and two low-cost optical particle counters (OPC; Alphasense OPC-N3 packaged into QuantAQ-MODULAIR-PM). This was done to correlate the particle concentration measurements for the lower-accuracy OPCs, which were available for the duration of the yearlong study, with the higher accuracy APS, which was only available intermittently. Kaur and Kelly evaluated nine Alphasense OPC-N3 sensors and reported a negative bias for particle concentration relative to the APS, as well as substantial inter-sensor variability.[19] Since CADR is calculated based on the change in particle concentration over time, an error in absolute sensor accuracy (*i.e.* gain) does not impact the results. However, sensor non-linearity does impact the results and is important to correct for.

As described in the ESI,† the particle aerodynamic diameters defining each APS bin were converted to physical diameter (assuming spherical particles) to account for particle density and aligned with the optical diameter bins for the OPC. A set of empirical correlations were then developed to convert OPC particle concentrations to APS-equivalent particle concentrations. The APS-equivalent values were then used to calculate the air changes per hour (ACH) for particle removal (bins 0–6) as described by Dal Porto *et al.* for the CR box including filtration (f), deposition (d), and infiltration (i), termed ACH_{f+d+i}.[3] Particle removal by deposition may be enhanced by the increased turbulence engendered by the fan on the CR box, enhancing the apparent losses due to filtration alone. We distinguish below between depositional losses with (d + fan) and without (d) the CR box fan.

Curve fits were calculated with Igor Pro v9.02 using the Levenberg–Marquardt least-squares method. The 95% confidence interval for each fit coefficient for ACH_{f+d+i} is also reported.

The air changes per hour (ACH) for deposition (d) and infiltration (i), termed ACH_{d+i}, was measured in an experiment in the conference room where:

1. Salt particles were generated for 10 minutes. Two fans placed on the table mixed the room air at low speed during this period.

2. The mixing fans were turned off. The room was left undisturbed for 24 hours.

The APS-equivalent values were then used to calculate for particle removal as described by Dal Porto *et al.*[3] Particle concentrations for larger particle diameters dropped below the detection limit of the OPC before the end of the 24 hour settling period. The particle loss rate analysis was limited to the period where the particle concentration was above 0. The particle loss rate for deposition and infiltration and analysis period for each

Table 2 Particle loss rates from deposition and infiltration by particle size

Bin (j)	APS physical diameter (μm)	OPC optical diameter (μm)	ACH_{i+d} (h^{-1})	Analysis period (h)
0	≤0.46	0.35–0.46	0.141	24.0
1	0.46–0.66	0.46–0.66	0.166	24.0
2	0.66–1.03	0.66–1.0	0.202	21.7
3	1.03–1.28	1.0–1.3	0.245	14.7
4	1.28–1.72	1.3–1.7	0.284	12.0
5	1.72–2.30	1.7–2.3	0.378	6.5
6	2.30–3.07	2.3–3.0	0.523	1.9

bin are shown in Table 2. As generally expected, ACH_{d+i} increased with particle size.

The CADR for the air cleaner for each particle size bin "j" was then calculated from eqn (1):

$$CADR_{(j)} = (ACH_{f+d+i(j)} - ACH_{d+i(j)})V \quad (1)$$

where V is the volume of the conference room (120 m^3). The 95% confidence interval for each $ACH_{f+d+i(j)}$ was used to estimate the confidence interval for $CADR_{(j)}$. Although there are also uncertainties in calculation of $ACH_{d+i(j)}$ and V, these values were only measured once and were held constant in the long-term performance analysis. Therefore, uncertainties in these values do not impact the analysis of the change in performance of the CADR boxes over time. Note that the CADR obtained from eqn (1) includes the combined effects of removal by the filter and enhanced depositional losses.

To simplify the presentation of the data, the CADR results from bins 0 to 6 were averaged into two groups: particles with optical diameter less than 1 μm (more representative of particle diameters observed in wildfire smoke) and particles with optical diameters between 1 to 3 μm (more representative of particle diameters observed in infectious respiratory aerosols).[20,21] The average CADR for all bins was also calculated. All averaging calculations weighted the CADR measurement for each bin equally. To estimate the uncertainty of the CADR measurement method, we measured the CADR of box 3 on speed high 10 times. This testing was performed after the 40 week deployment. The repeat measurements included setup and takedown of the CR box and the instrumentation to account for minor differences in placement. The uncertainty (two standard deviations) was 6% of the average measurement for 0.35 to 1 μm optical diameter particles and 5% for 1 to 3 optical diameter particles. This uncertainty (as a percentage) was applied to all CADR measurements.

Single pass filtration efficiency and pressure drop

The single pass filtration efficiency of the air filters for each particle size bin "j" was calculated with eqn (2):

$$SPFE_{(j)} = \left(\frac{C_{\text{filter inlet}(j)} - C_{\text{filter outlet}(j)}}{C_{\text{filter inlet}(j)}}\right) \quad (2)$$

where $C_{\text{filter inlet}}$ is the particle concentration in the room as measured by OPC-1 and $C_{\text{filter outlet}}$ is the particle concentration inside the CR box as measured simultaneously by OPC-2. OPC-2 was placed inside the filter box by cutting an access door in the cardboard bottom and taping the door shut during testing. Both OPC-1 and OPC-2 were sampled every 5 s for 2 min and the average result was calculated. The average OPC measurements were converted to equivalent APS values prior to calculation of the SPFE with eqn (2). Static pressure drop across the filters was measured using plastic tubing and a differential pressure sensor (The Energy Conservatory DG-500).

While the SPFE and pressure drop data were collected every 10 weeks, the sensor access door was unintentionally not taped during SPFE testing that occurred on weeks 10 and 20. Leaks in the bottom of the box made the results unreliable and therefore only SPFE results from 0, 30, and 40 weeks are presented. The access door was securely taped for the CADR testing and those results were unaffected.

Enhanced particle deposition

As noted above, the air movement from the fan increases particle deposition by increasing the turbulent kinetic energy in the room.[22] While such enhanced loss is attributable to the CR box it is not attributable to removal by the filters. To separate particle removal by the filter from enhanced deposition we followed the same procedure as used to measure the ACH_{d+i} but with a "mock" CR box that had the fan in the same orientation as a standard CR box but with the filters removed. The resulting loss rate, $ACH_{d+i,\ fan(j)}$, includes the enhanced particle deposition of the CR box fan (Table 3). As expected, the $ACH_{d+i+fan(j)}$ values at all sizes exceeded the ACH_{d+i} values.

A modified $CADR_{filter}$, meaning the CADR attributed to the filters only, was calculated from eqn (3):

$$CADR_{filter_{(j)}} = (ACH_{f+d+i(j)} - ACH_{d+i+fan(j)})V \quad (3)$$

Table 3 Particle loss rates from deposition and infiltration with box fan on (no filter) by particle size

Bin (j)	OPC optical diameter (μm)	Low speed (h^{-1})	Medium speed (h^{-1})	High speed (h^{-1})	Analysis period (h)
0	0.35–0.46	0.44	0.37	0.55	2.0
1	0.46–0.66	0.68	0.60	0.76	2.0
2	0.66–1.0	0.79	0.72	0.89	2.0
3	1.0–1.3	0.91	0.86	1.06	2.0
4	1.3–1.7	1.02	0.97	1.17	2.0
5	1.7–2.3	1.17	1.17	1.35	2.0
6	2.3–3.0	1.38	1.58	1.69	0.6–0.9

Total airflow rate

Airflow rate of the fan was analysed over the 40 weeks of testing to determine if performance losses were attributed to a reduction in filtration efficiency and/or a reduction in total fan flow rate (due to increased resistance to flow as filters accumulated particulate matter). The total airflow rate of the fan, Q, was estimated from the $CADR_{filter}$ divided by the SPFE for each bin "j".

$$Q_{(j)} = (CADR_{filter_{(j)}}/SPFE_{(j)}) \quad (4)$$

The $CADR_{filter}$ values were used here instead of the CADR values so as to focus on just the airflow through the filters. The calculated flow rate for a CR box should be the same across all particle size bins. Any size-dependent differences in the flow result are attributed to the uncertainty in the measurements of $CADR_{filter}$ and SPFE. The average flow rate ($\bar{Q}$) was calculated as the average across all seven size bins. The 95% confidence interval was calculated as two standard deviations across the seven measurements.

Estimate of mass collected on filters

Indoor air particle concentrations in each space with a CR box deployed were monitored with a low-cost Purple Air sensor (PA-II-SD) that reported an average result from two Plantower PMS5003 nephelometers. Nephelometers measure total light scattered by an air sample and estimate the total particle mass concentration.[23] Since the CR box will collect particles of all sizes, the Purple Air signal for particulate matter less than 10 μm (PM_{10}) was used, which is the best measurement available from these low-cost sensors to represent the total particle mass concentration of the air being filtered. While a field evaluation by the South Coast Air Quality Management District determined outdoor PM_{10} measured by Purple Sensors was only moderately correlated ($R^2 < 0.41$) with PM_{10} measured by federal equivalent reference methods, the study of six sensors showed good agreement between devices.[24] Relevant to indoor environments, it has also been demonstrated that Purple Air PM_{10} measurement accuracy varies substantially and depends on the source of indoor particles; the accuracy generally decreases as particle size and concentration increase.[25,26] While the spaces monitored in our study had similar sources of outdoor particles due to their proximity on the same campus, the two laboratories had different sources of indoor particles. Low accuracy of the nephelometer-based PM_{10} measurements, and lack of a true mass-based PM_{10} reference measurement, is a limitation of this study and thus the cumulative mass is labelled as "estimated" to indicate the accuracy limitation of the sensors used.

The mass deposited on the filters over each deployment period was estimated per eqn (4). For each fan speed i, the cumulative mass deposited was estimated by multiplying the number of hours (t) of operation (as measured by the power meter), the average particle mass concentration as measured by Purple Air ($\overline{PM_{10}}$), and the average CADR for all particle bins ($\overline{CADR}$). The total estimated mass was calculated as the sum of the mass collected at each fan speed (low, medium, high). These data were used to estimate the cumulative mass deposited on the box at the time each set of CADR and SPFE measurements were taken.

$$m_{total} = \sum_{i=low}^{high} \overline{CADR_i} \times \overline{PM_{10i}} \times t_i \quad (5)$$

Results & discussion

Power

The complete power data collected for each box fan are included in the ESI in Fig. S3† and the total hours of operation for each box fan by speed are summed in Table 5. CR boxes 2 and 3 ran as expected during the entire study. Run hours for boxes 1 and 4 were approximately 10% and 2% less, respectively, due to the boxes becoming unintentionally unplugged. The initial power and final power for each box fan were estimated using a linear fit of the power data collected at the speed used most frequently (Table 4). For box 2, power data did not log during the final deployment period (although the fan was running per periodic observations), so the final power was predicted based extrapolation of the measurements from the first three deployment periods and an additional day of power measurements collected at the end of the experiments. Overall, changes in power were small and, for boxes 1, 3, and 4, were within the accuracy specification of the power meter. Box 2 measurements showed a power decrease of about 3 W, potentially indicating that the airflow through the fan was slightly reduced.

Clean air delivery rate

The average CADR for the size bin as a function of the estimated cumulative mass deposited on the filter is plotted in Fig. 2 for high, medium, and low fan speeds. As a reminder, the CADR values include the combined effects of removal by the filters and enhanced depositional losses. Complete CADR results for each particle diameter bin are available in the ESI (Tables S4 to S6†). Further details about the cumulative mass results displayed on the x-axis are provided in the next section. Note that particle accumulation combines the effects of operating time with the average particle concentration; here, an increase in particle accumulation for a given box corresponds to an increasing overall deployment time.

Overall the CADR measurements (and associated cost-effectiveness) for new CR boxes (514 to 1387 $m^3\ h^{-1}$, depending on box, fan speed, and particle size) were within range of others reported in the literature (Fig. 2).[18] Box 1 (AH filters) outperformed the other CR boxes, both when new and throughout the study. This illustrates that filter selection, even

Table 4 Initial power and final power for each box fan estimated using a linear fit of the power data collected at the most used speed

Box	Main speed	Initial power (W)	Final power (W)	% change
1	Medium	72.6	73.3	1.0%
2	Low	63.2	60.3	−4.5%
3	High	86.5	87.1	0.7%
4	Low	60.1	60.3	0.4%

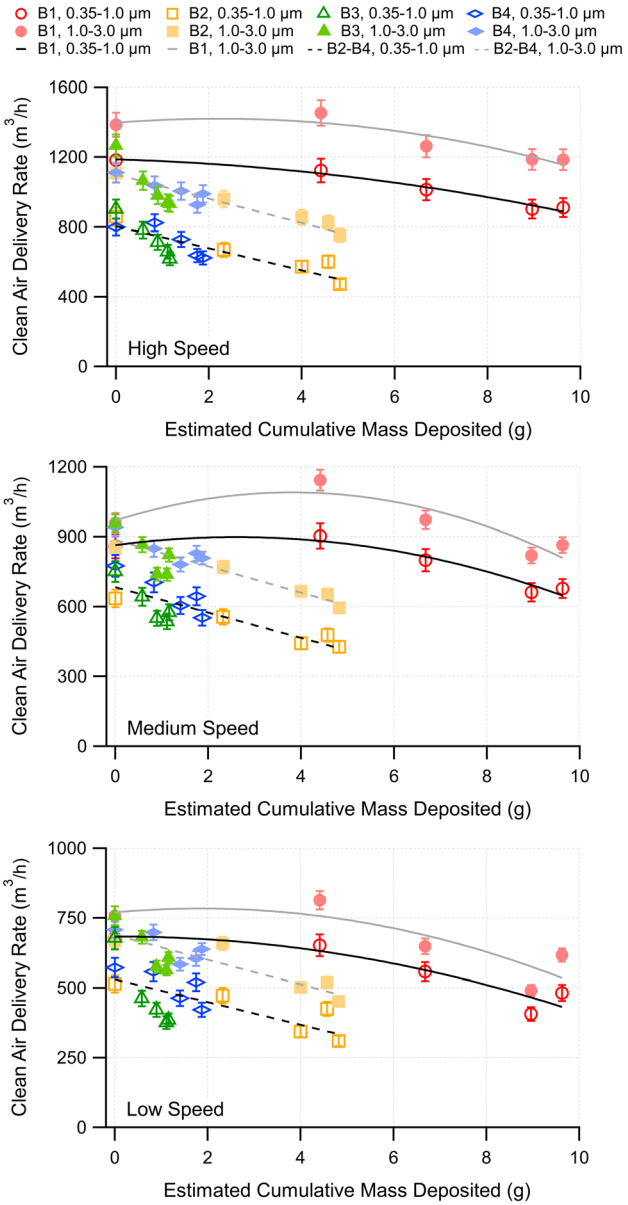

Fig. 2 CADR results for CR boxes as a function of cumulative mass deposited over the 40 week field trial. Coefficients for the linear and quadratic fits are provided in Tables S2 and S3.† Error bars represent an estimated uncertainty of 6% for 0.35 to 1 μm optical diameter particles and 5% for 1 to 3 optical diameter particles.

among those rated MERV 13, may impact performance. In addition to differences in box fans, filter selection likely contributes to the wide range of CADR results reported in the literature.[18] In addition to actual differences in CR box performance due to material selection, measurement methods will influence results because of CADR dependence on particle size. For example, use of sensors and methods that calculate CADR based on particle mass removal rates (as opposed to particle count removal rates) are likely to yield higher CADR results because MERV 13 filters have higher removal rates of larger particles that dominate mass-based measurements.

This study was designed to assess the long-term performance of CR boxes and was not designed to assess differences between MERV 13 filter brands, and we did not expect the results to be different for the box built with a different brand of filter. The minimum 0.3 to 1.0 μm diameter particle removal efficiency must be at least 50% for MERV 13 filters and 75% for MERV 14 filters. The large jump in filtration efficiency between MERV 13 and MERV 14 shows that there could be variation among MERV 13 filters brands that meet or exceed the MERV 13 standard but are still classified as such.[27] Both types of filters used in this study met requirements of MERV 13 filters, with a small difference between the filters' initial filtration efficiency (*e.g.* AH 61% and TA 55% for 0.3 to 1.0 μm particles) per the ASHRAE 52.2-2017 test reports, which were obtained from the manufacturers.[28,29] Although initial filtration efficiency differences were small, CR box builders may benefit from reviewing manufacturer provided filtration performance data when making filter selection instead of only considering MERV rating (in addition to consideration of filter cost).

As expected for MERV 13 filters, the CADR for 1.0–3.0 μm optical diameter particles was consistently higher than the CADR for 0.35–1.0 μm optical diameter particles because they are more easily removed by impaction with filter fibres.[30] Across four CR boxes tested at three speeds at five times during the 40 week deployment ($n = 60$), the CADR for 1.0–3.0 μm optical diameter particles was, on average, 34% higher than the CADR for 0.35–1.0 μm optical diameter particles.

The CADR for CR boxes 2, 3, and 4 (TA filters) declined approximately linearly with particle accumulation on the filters (Fig. 2). Considering these three CR boxes as one dataset, a linear least-squares regression estimated that, after 4.8 g of particles was deposited, the CADR was 62–63% of the new CR box performance for particles 0.35 to 1.0 μm optical diameter and 69–70% of the new CR box performance for particles 1.0 to 3.0 μm optical diameter.

The CADR for CR box 1 was higher than CR boxes 2, 3, and 4. A two-sample *t*-test comparing all CADR measurements for box 1 to all CADR measurements for box 2, 3, and 4 (at the same speed) determined that the higher value of CADR for box 1 was statistically significant at high speed ($p = 6.6 \times 10^{-7}$) and medium speed ($p = 1.5 \times 10^{-3}$) but not at low speed ($p = 0.20$). Coincidentally, box 1 was deployed in the dustiest environment and accumulated an estimated 9.6 g of particles on the filters over the course of the deployment. Box 1 appeared to have an increase in CADR in almost all cases between the first and second measurements (except high speed, 0.35 to 1.0 μm optical diameter particles). CADR generally decreased in subsequent measurements. A quadratic least-squares regression estimated that, after 9.6 g of particles was deposited, the CADR was 63–75% of the new CR box performance for particles 0.35 to 1.0 μm optical diameter and 70–84% of the new CR box performance for particles 1.0 to 3.0 μm optical diameter. CADR was better maintained at high and medium speed than low speed. The sample size of one box with AH filters is too limited to draw general conclusions; it is unknown if a larger sample size would exhibit similar behaviour.

Table 5 Hours of operation at each speed for each deployment period for each CR box. The average CADR was calculated as the average of the measurements taken before and after the deployment period. The average PM10 measurement during each period is reported as well as the estimated amount of particle mass deposited. *Power measurements did not log for box 2, deployment period 4. Hours of operation were calculated from the programmable timer schedule and observations that the CR box as working as expected

CR box	Deployment period	Hours of operation	Speed	$\overline{\text{CADR}}$ ($m^3\ h^{-1}$)	Average PM_{10} ($\mu g\ m^{-3}$)	PM_{10} 10th percentile ($\mu g\ m^{-3}$)	PM_{10} 90th percentile ($\mu g\ m^{-3}$)	% PM_{10} data available	Estimated PM_{10} deposited (g)	Estimated cumulative PM_{10} deposited (g)
1	1	639	Medium	978	7.05	2.21	13.24	45%	4.41	4.41
	2	63	Medium	969	2.15	0.06	2.55	100%	0.13	4.54
		585	Low	677	5.41	0.47	11.48	73%	2.14	6.68
	3	369	Medium	825	5.14	0.06	13.81	100%	1.57	8.25
		261	Low	555	4.94	0.20	11.55	100%	0.72	8.96
	4	432	Medium	768	2.00	0.05	7.26	25%	0.66	9.63
Total box 1		2349								9.6
2	1	639	Low	591	6.14	1.08	12.13	100%	2.43	2.32
	2	648	Low	507	5.14	0.31	10.56	100%	1.69	4.00
	3	630	Low	456	1.98	0.04	5.66	100%	0.57	4.57
	4	693	Low*	435	0.83	0.03	1.80	100%	0.25	4.82
Total box 2		2610								4.8
3	1	297	Medium	820	0.92	0.05	2.19	100%	0.22	0.22
	1	342	High	1027	1.02	0.03	1.96	92%	0.45	0.58
	2	648	High	904	0.54	0.00	1.48	100%	0.32	0.90
	3	459	High	842	0.45	0.00	1.24	100%	0.17	1.07
		171	Medium	654	0.35	0.00	1.14	100%	0.04	1.11
	4	135	Medium	683	0.18	0.00	0.44	100%	0.02	1.13
		558	High	808	0.07	0.00	0.19	100%	0.03	1.16
Total box 3		2610								1.2
4	1	639	Low	644	2.01	0.11	4.54	100%	0.94	0.83
	2	648	Low	585	1.52	0.05	3.66	100%	0.57	1.40
	3	576	Low	550	1.09	0.01	3.28	100%	0.34	1.75
	4	693	Low	557	0.30	0.01	0.91	100%	0.12	1.87
Total box 4		2556								1.9

Analysis of the CADR results alone cannot determine if the CADR is decreasing due to a loss of filtration efficiency or due to a reduction in flow rate due to increased resistance of the filters. The SPFE measurements, flow rate calculations, and power measurements provide insight to the reasons for the performance decrease.

Cumulative mass deposited

For each CR box and deployment period, the hours of operation at each speed, the average CADR calculated for that speed (from Fig. 2), the average PM_{10} measurement during that period and speed, and the PM_{10} deposited are detailed in Table 5. In some instances, periods of PM_{10} data were missing due to loss of sensor power (Table 5). The average PM_{10} measurement was calculated from the available data and was used as the average for the deployment period. Box 1, which had a higher CADR than the other boxes and was placed in a lab environment with sources of particle generation, accumulated the highest amount of estimated particle mass of 9.6 g over the 40 weeks of measurement. Box 2, which was also placed in a lab environment with sources of particle generation, accumulated an estimated particle mass of 4.8 g. Boxes 3 and 4, which operated in cleaner office environments, accumulated an estimated particle mass of 1 and 2 g respectively. Photographs of the filters at the end of the study are shown in Fig. 3.

Single pass filtration efficiency

The average SPFE as a function of the estimated cumulative mass deposited on the filter is plotted in Fig. 4 for high, medium, and low fan speeds. Complete SPFE results for each particle diameter bin are available in the ESI (Tables S7 to S9†). In agreement with the CADR measurements, the SPFE for the 1.0–3.0 μm optical diameter particles was consistently higher than for 0.35–1.0 μm optical diameter particles because larger

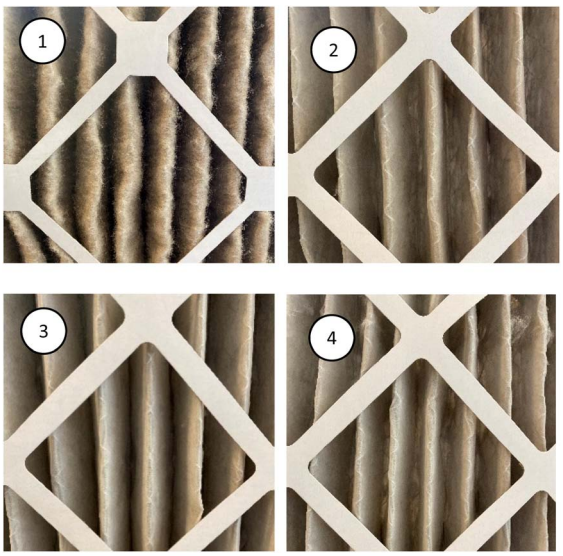

Fig. 3 Photographs of filters for each CR box at the end of the last deployment period.

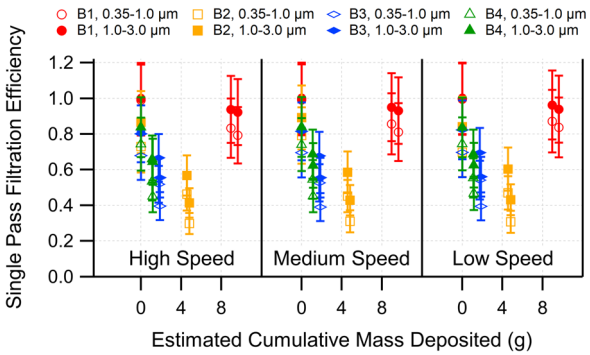

Fig. 4 SPFE results for CR boxes as a function of cumulative mass deposited at 0, 30, and 40 weeks. Error bars represent an estimate 20% relative error on the SPFE measurement.

particles are more easily removed by impaction with filter fibres. Across four CR boxes tested at three speeds at five times during the 40 week deployment ($n = 60$), the SPFE for 1.0–3.0 μm optical diameter particles was, on average, 23% higher than the SPFE for 0.35–1.0 μm optical diameter particles. It is difficult to estimate the uncertainty of the SPFE measurements (which are more sensitive to accurate measurement of absolute particle concentration than the CADR measurements). Assuming a best-case scenario where the measured particle concentrations have an accuracy of ±10% of reading (which is the reported accuracy of the APS), uncertainty propagation of the SPFE formula is a 20% relative uncertainty. While there is substantial uncertainty in these measurements, the results are still helpful to understand the change in CR box performance over time.

The SPFE for CR box 1 was consistently higher than CR boxes 2, 3, and 4. The SPFE declined over time for all boxes. A contradiction in the data is an apparent increase in CADR for box 1 between the first and second measurements along with an initial SPFE of nearly 1 (SPFE was not measured at the second test period). An increase in CADR would occur from either an increase in filtration efficiency or an increase in airflow through the filter. There is no physical rationale for an increase in airflow over time, as the fan motor was unchanged, and filter resistance increased with time (see sections on power and total airflow rate and pressure drop). Likewise, if SPFE started at the maximum of 1 as observed, it would be impossible to increase. Therefore, the remaining explanations for the results observed are error in the SPFE measurement (such that the measured value is higher than actual) or error in the CADR measurement (such that the difference between the first and second measurement is not significant). Larger sample sizes would be needed to investigate this further. While we applied a quadratic fit to the box 1 results to help visualize the observation, we do not intend to imply the observed increase in CADR is statistically significant.

Collectively for CR boxes 2, 3, and 4, the decline in SPFE was correlated with the cumulative mass deposited. This likely results from the filters having an initial electrostatic effect that is reduced as the filter accumulates particles.[31] Both manufacturers confirmed that the filters use both charged fibres and

mechanical principles to remove particles. ASHRAE 52.2 testing that is used to determine MERV rating does not take into account electrostatic discharge. The difference in the SPFE between the CR boxes indicates that box 1 filters may rely less on initial electrostatic forces to meet their stated initial MERV performance (since the box 1 removal efficiency better persists with particle accumulation). Unfortunately, performance data after electrostatic discharge are not generally available to the consumer in ASHRAE 52.2 test reports (unless optional appendix J is used).

Total airflow rate and pressure drop

For each test, there was substantial variation in the derived flow rates between the 7 particle size bins owing to the variability and uncertainty in the SPFE measurement (ESI, Tables S10 to S12†). This leads to relatively large standard deviations for each average flow rate determination (Fig. 5). Nonetheless, there is no strong indication that the flow rates decreased appreciably over time for any of the fans. In comparison, there were clearer trends in loss of SPFE with particle accumulation, particularly for boxes 2 to 4. This suggests that the declines in CADR over time are likely not due to a change in airflow, but rather due to a loss of filtration efficiency. This is counterintuitive to the expectation that the accumulation of particles will increase resistance on the filters and reduce airflow. MERV filters for HVAC applications are generally designed for an air velocity of 2.5 m s^{-1}, whereas the air velocity of the CR box (with approximately 1 m^2 of surface area) is 0.1 to 0.4 m s^{-1} for airflow rates of 500 to 1500 m^3 h^{-1}.

Complete pressure drop measurements are available in the ESI, Table S13.† At high speed, the static pressure drop across new boxes was 7.1 to 7.2 Pa and the final pressure drop was 8.2 to 10.9 Pa, where the highest final pressure drop was observed for box 1. This increase in pressure is small relative to the total external static pressure across the fan. For example, an increase of static pressure of 3 Pa at a flow rate of 1500 m^3 h^{-1} is equal to a fluid power loss of only 1.3 W. Although the efficiency of the fan and motor assembly is not known (so conversion to electrical power cannot be estimated), 1.3 W is small compared to the electrical input of the box fan at high speed (86 W).

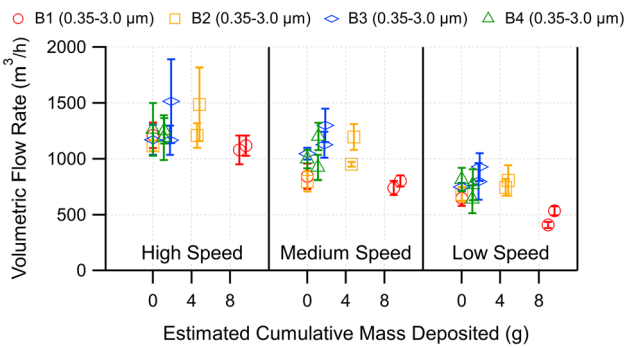

Fig. 5 Calculated flow results for CR boxes as a function of cumulative mass deposited at 0, 30, and 40 weeks. Error bars represent the 95% confidence interval for the average result calculated from 7 particle size bins for each test.

Therefore, while particle accumulation on the filters will increase resistance, the change is small relative to the external static pressure across the fan system and thus is expected to have minimal impact on total flow rate.

Limitations

This study had several limitations that should be considered in interpretation of the results and conclusions. It was designed to assess the long-term performance of CR boxes and was not designed to assess differences between MERV 13 filter brands. We did not expect the results to be different for the box built with a different brand of filters. While a clear difference was observed, the sample size of one box with AH filters is too limited to draw general conclusions; it is unknown if a larger sample size would exhibit similar behaviour. A study with larger sample sizes of CR boxes built with different filter brands could explore this further.

A second limitation was the estimate of PM_{10} cumulative mass. This metric was used to provide more information than the cumulative runtime because particle concentrations in the indoor environment vary widely. As discussed in the methodology, low-cost Purple Air sensors have only moderate correlation with PM_{10} reference measurements. An improvement to this study methodology would be to deploy periodic PM_{10} reference instruments (*e.g.* 1 week per deployment period) to calibrate the Purple Air sensors for the specific environments in which they are deployed.

Finally, in this study we did not directly measure airflow through the CR box. Methods that measure air velocity are challenging because they require many individual measurements and assumptions on the applicable area for the measured velocity to calculate flow.[3] As such, we estimated airflow as the ratio of measured CADR and SPFE. A limitation of this approach is a high uncertainty of the SPFE measurement, which impacts uncertainty of the total flow calculation.

Conclusions

Four CR boxes deployed across a university campus in labs and offices demonstrated robust performance over 40 weeks of operation. Across four CR boxes tested at three speeds at five times during the deployment ($n = 60$), the CADR for 1.0–3.0 μm optical diameter particles was, on average, 34% higher than the CADR for 0.35–1.0 μm optical diameter particles. This result is consistent with rating requirements for MERV 13 filters. While CR boxes are effective at filtering all particle sizes, the results show they are particularly well suited for filtering most of the volume of respiratory aerosol particles. Programmable timers are a useful tool to efficiently operate the CR boxes automatically when people are expected to be present.

Considering all three boxes with the same filter brand (TA) as one dataset, a linear least-squares regression estimated that, after 4.8 g of particles were deposited, the CADR was 62–63% of its initial value for particles 0.35 to 1.0 μm optical diameter and 69–70% of its initial value for particles 1.0 to 3.0 μm optical diameter. For the CR box with a different filter brand (AH),

a quadratic least squares regression estimated that, after 9.6 g of particles deposited, the CADR was 63–75% of its initial value for particles of 0.35 to 1.0 μm optical diameter and 70–84% of its initial value for particles 1.0 to 3.0 μm optical diameter. Since CR boxes are an order of magnitude less in cost than HEPA filters and they maintain at least 60% of their initial CADR (even after 40 weeks of daily operation in dirty lab environments), they are a cost-effective long-term tool to manage air quality. The results indicate that annual filter replacements are sufficient in dirty environments and that filters may last 2–3 years in clean office environments. No substantial wildfire smoke was observed during the study period. A study by Liang *et al.* quantified that indoor air PM2.5 was approximately 2.7 times higher on "fire days" *versus* "non-fire days".[32] Thus, the occasional and short-term presence of wildfire smoke is not expected to appreciably affect the 1–3 year lifetime of the CR box.

Performance losses as particles accumulated were attributed to loss of single pass filtration efficiency (likely due to loss of initial electrostatic charge on the filters). Although total airflow rate measurements had high uncertainty, there were no indications that minimally increased filtration resistance significantly affected airflow, even for CR boxes operating in laboratory environments with sources of particle generation.

Data availability

All data needed to evaluate the conclusions in the article are present in the article and/or the ESI.†

Author contributions

RLC conceptualized the experiment. TP, RLC, and CDC developed the methodology. TP and GJ conducted the investigation and the formal analysis. GJ was responsible for programming and visualization. RLC and CDC provided supervision. TP wrote the original draft. All authors contributed to review and editing.

Conflicts of interest

There are no conflicts to declare.

Acknowledgements

The authors greatly appreciate the contributions from students in ECI/ATM 149 at UC Davis, who performed the fourth round of testing. Paul Fortunato is thanked for drawing the graphic of the Corsi–Rosenthal box. Funding for this study was provided internally by the University of California, Davis.

References

1 E. Cheek, V. Guercio, C. Shrubsole and S. Dimitroulopoulou, Portable air purification: review of impacts on indoor air quality and health, *Sci. Total Environ.*, 2021, **766**, 142585.
2 International Standards Organization, *ISO 29463-5:2022 High-Efficiency Filters And Filter Media For Removing Particles In Air*, 2022.
3 R. Dal Porto, M. N. Kunz, T. Pistochini, R. L. Corsi and C. D. Cappa, Characterizing the performance of a do-it-yourself (DIY) box fan air filter, *Aerosol Sci. Technol.*, 2022, **56**, 564–572.
4 Association of Home Appliance Manufacturers, *Method for Measuring Performance of Portable Household Electric Room Air Cleaners*, 2020.
5 N. T. Myers, R. J. Laumbach, K. G. Black, P. Ohman-Strickland, S. Alimokhtari, A. Legard, A. De Resende, L. Calderon, F. T. Lu, G. Mainelis and H. M. Kipen, Portable air cleaners and residential exposure to SARS-CoV-2 aerosols: a real-world study, *Indoor Air*, 2022, **32**, e13029.
6 K. L. Buising, R. Schofield, L. Irving, M. Keywood, A. Stevens, N. Keogh, G. Skidmore, I. Wadlow, K. Kevin, B. Rismanchi, A. J. Wheeler, R. S. Humphries, M. Kainer, J. Monty, F. McGain and C. Marshall, Use of portable air cleaners to reduce aerosol transmission on a hospital coronavirus disease 2019 (COVID-19) ward, *Infect. Control Hosp. Epidemiol.*, 2022, **43**, 987–992.
7 N. Banholzer, K. Zurcher, P. Jent, P. Bittel, L. Furrer, M. Egger, T. Hascher and L. Fenner, SARS-CoV-2 transmission with and without mask wearing or air cleaners in schools in Switzerland: a modeling study of epidemiological, environmental, and molecular data, *PLoS Med.*, 2023, **20**, e1004226.
8 V. A. Vartiainen, J. Hela, A. Luoto, P. Nikuri, E. Sanmark, A. Taipale, I. Ehder-Gahm, N. Lastovets, P. Sormunen, I. Kulmala and A. Säämänen, The effect of room air cleaners on infection control in day care centres, *Indoor Environments*, 2024, **1**, 100007.
9 T. Pistochini, C. Mande and S. Chakraborty, Modeling impacts of ventilation and filtration methods on energy use and airborne disease transmission in classrooms, *J. Build. Eng.*, 2022, **57**, 104840.
10 R. W. Allen, C. Carlsten, B. Karlen, S. Leckie, S. van Eeden, S. Vedal, I. Wong and M. Brauer, An Air Filter Intervention Study of Endothelial Function among Healthy Adults in a Woodsmoke-impacted Community, *Am. J. Respir. Crit. Care Med.*, 2011, **183**, 1222–1230.
11 E. V. Bräuner, L. Forchhammer, P. Moller, L. Barregard, L. Gunnarsen, A. Afshari, P. Wåhlin, M. Glasius, L. O. Dragsted, S. Basu, O. Raaschou-Nielsen and S. Loft, Indoor particles affect vascular function in the aged: an air filtration-based intervention study, *Am. J. Respir. Crit. Care Med.*, 2008, **177**, 419–425.
12 W. J. Fisk and W. R. Chan, Health benefits and costs of filtration interventions that reduce indoor exposure to PM2.5 during wildfires, *Indoor Air*, 2017, **27**, 191–204.
13 Association of Home Appliance Manufacturers, *Find a Certified Room Air Cleaner*, **https://ahamverifide.org/directory-of-air-cleaners/**, accessed June 24, 2024.
14 A. L. Holder, H. S. Halliday and L. Virtaranta, Impact of do-it-yourself air cleaner design on the reduction of simulated wildfire smoke in a controlled chamber environment, *Indoor Air*, 2022, **32**, e13163.
15 D. Srikrishna, Can 10× cheaper, lower-efficiency particulate air filters and box fans complement High-Efficiency

Particulate Air (HEPA) purifiers to help control the COVID-19 pandemic?, *Sci. Total Environ.*, 2022, **838**, 155884.
16 R. C. Derk, J. P. Coyle, W. G. Lindsley, F. M. Blachere, A. R. Lemons, S. K. Service, S. B. Martin, Jr, K. R. Mead, S. A. Fotta, J. S. Reynolds, W. G. McKinney, E. W. Sinsel, D. H. Beezhold and J. D. Noti, Efficacy of Do-It-Yourself air filtration units in reducing exposure to simulated respiratory aerosols, *Build. Environ.*, 2023, **229**, 109920.
17 N. T. Myers, K. P. Dillon, T. T. Han and G. Mainelis, Performance evaluation of different low-cost DIY air cleaner configurations, *Aerosol Sci. Technol.*, 2023, **57**, 1128–1141.
18 M. L. Jehn, J. M. Andino, B. Russell, V. Rana, S. Akter, M. A. Creed, H. Sodhi, B. Holmes, T. Palit, J. Wani and K. Wagstrom, Effectiveness of do-it-yourself air cleaners in reducing exposure to respiratory aerosols in US classrooms: a longitudinal study of public schools, *Build. Environ.*, 2024, **258**, 111603.
19 K. Kaur and K. E. Kelly, Laboratory evaluation of the Alphasense OPC-N3, and the Plantower PMS5003 and PMS6003 sensors, *J. Aerosol Sci.*, 2023, **171**, 106181.
20 T. L. Sparks and J. Wagner, Composition of particulate matter during a wildfire smoke episode in an urban area, *Aerosol Sci. Technol.*, 2021, **55**, 734–747.
21 M. Alsved, D. Nygren, S. Thuresson, C. J. Fraenkel, P. Medstrand and J. Löndahl, Size distribution of exhaled aerosol particles containing SARS-CoV-2 RNA, *Infect. Dis.*, 2023, **55**, 158–163.
22 T. L. Thatcher, A. C. K. Lai, R. Moreno-Jackson, R. G. Sextro and W. W. Nazaroff, Effects of room furnishings and air speed on particle deposition rates indoors, *Atmos. Environ.*, 2002, **36**, 1811–1819.
23 D. H. Hagan and J. H. Kroll, Assessing the accuracy of low-cost optical particle sensors using a physics-based approach, *Atmos. Meas. Tech.*, 2020, **13**, 6343–6355.
24 South Coast Air Quality Management District, *Field Evaluation Purple Air (PA-II) PM Sensor*, 2017.
25 Z. Wang, W. W. Delp and B. C. Singer, Performance of low-cost indoor air quality monitors for PM2.5 and PM10 from residential sources, *Building and Environment*, 2020, **171**, 106654.
26 S. Park, S. Lee, M. Yeo and D. Rim, Field and laboratory evaluation of Purple Air low-cost aerosol sensors in monitoring indoor airborne particles, *Building and Environment*, 2023, **234**, 110127.
27 American Society of Heating Refrigerating and Air-Conditioning Engineers, *ANSI/ASHRAE Standard 52.2-2017*, 2017.
28 N. Adams, *ASHRAE 52.2-2017 Test Report for Air Handler 2EKJ5 Obtained from*nadams@aafintl.com.
29 J. Rosenthal, *ASHRAE 52.2-2017 Test Report for Tex-Air Filter Obtained from*jimrosenthal5757@aol.com.
30 W. J. Kowalski and W. P. Bahnfleth, *MERV Filter Models for Aerobiological Applications*, 2002.
31 J. E. Yit, B. T. Chew and Y. H. Yau, A review of air filter test standards for particulate matter of general ventilation, *Build. Serv. Eng. Res. Tecnol.*, 2020, **41**, 758–771.
32 Y. Liang, D. Sengupta, M. J. Campmier, D. M. Lunderberg, J. S. Apte and A. H. Goldstein, Wildfire smoke impacts on indoor air quality assessed using crowdsourced data in California, *Proc. Natl. Acad. Sci. U. S. A.*, 2021, **118**, e2106478118.